

## **A NOVEL COUPLED T-MATRIX AND MICROWAVE NETWORK APPROACH FOR MULTIPLE SCATTERING FROM PARALLEL SEMICIRCULAR CHANNELS WITH ECCENTRIC CYLINDRICAL INCLUSIONS**

**Y.-J. Zhang, A. Bauer, and E.-P. Li**

Computational Electromagnetics and Electronics  
Institute of High Performance Computing  
Singapore 117528

**Abstract**—A novel coupled T-matrix and microwave network approach is proposed for the multiple scattering from parallel semicircular channels. First, an equivalent network is set up to derive the T-matrix of a single channel, in which the S-parameters are derived for the semicircular boundary and the T-matrix of the inclusive cylinders is served as loading matrix of s-parameters. In addition, the T-matrix of the inclusive cylinders is obtained from the T-matrix of each cylinder in its local coordinates using the addition theorem of cylindrical harmonics. Thus, the T-matrix description of semicircular channels could be obtained steadily by the equivalent microwave network theory. Second, the addition theorems in half space are derived and utilized to take account of multiple scattering from several parallel channels. Comparing with previous dual-series eigenfunction solutions, the coupled method simplifies the analysis and could handle much more complex structures step by step. The method is verified by comparison with previous publications and both TM and TE wave illumination are considered.

### **1 Introduction**

### **2 Problem Description**

### **3 Microwave Network Approach for T-Matrix of Single Channel**

#### **3.1 S-Parameters Description of Semicircular Boundary**

#### **3.2 Aggregated T-Matrix of Multiple Circular Cylinders**

### **4 T-matrix Approach for Multiple Scattering from Parallel Channels**

## 5 Incident Wave Expansion and Far Field Calculation

## 6 Case Numerical Examples and Discussions

## 7 Conclusions

## References

### 1. INTRODUCTION

The channels, grooves and cracks in a ground plane have interesting electromagnetic scattering properties with applications in radar cross-section reduction and control, and thus have attracted extensive studies [1–7]. M. K. Hinders and A. D. Yaghjian provided exact dual-series eigenfunction solutions to a single semicircular channel [3] and the author of [5] extended the method to a semicircular channel with a coaxial circular cylinder inclusion. A similar method is adopted in [6, 7] for analysis of semielliptic channels using Mathieu function instead of cylindrical harmonics. Recently, the eigenfunction solutions (radial mode matching method) are applied in multiple scattering of two semicircular channels [8]. However, only TM wave is considered.

In this paper, we propose a novel approach for simulation of multiple scattering from parallel semicircular channels. Each channel could contain several cylindrical inclusions and either TM or TE wave incidences are discussed.

Although scattering from a circular cylinder with multiple cylindrical inclusions has been investigated by authors of [9, 10], to the best of our knowledge, the structure we intend to analyze here has not been simulated before. Moreover, to simplify the analysis of complex channel structures, a novel equivalent microwave network approach is first used to obtain the T-matrix of a single channel. Although T-matrix method is nothing new and has been extensively used in analysis of multiple scattering from 2D or 3D objects [11–14], to our knowledge, it has never been utilized in multiple scattering from parallel semicircular channels. To do so, instead of cylindrical or spherical harmonics in free space for 2D or 3D targets, the addition theorems of cylindrical harmonics in half space are derived and given explicitly. Then, an aggregated T-matrix of parallel channels could be obtained from the T-matrix of the individual channels. The scattering field could be evaluated easily by the aggregated T-matrix of parallel channels. In contrast to conventional eigenfunction solutions, which handle all sub-regions simultaneously, the coupled method proposed simplifies the analysis by adopting divide-and-conquer strategy and thus, is able to simulate very complicated channel structures step by

step.

This paper is organized as follows. In Section 2, a short problem description is given to illustrate the geometric structure we are going to simulate. The equivalent microwave network approach for T-matrix of a single channel will be discussed in Section 3. Section 4 describes the aggregated T-matrix method of parallel channels using addition theorems of cylindrical harmonics in half space. The formulas for incident waves and far field computation are provided in details in Section 5. Finally, numerical examples and discussions are given in Section 6 followed by a short conclusion.

## 2. PROBLEM DESCRIPTION

Let us consider parallel semicircular channels located in a conducting ground as shown in Fig. 1(a). The channels could have different radius and separations from each other. Fig. 1(b) gives the structure of a single channel as an example. It can be seen that this channel contains several circular metal or dielectric cylinders inside. The channel with relative dielectric constants  $(\mu_c, \varepsilon_c)$  is assumed to be embedded in a surrounding medium  $(\mu_a, \varepsilon_a)$ . The inclusive cylinders are located at  $(\rho_s, \varphi_s)$ , and its dielectric constants are denoted as  $(\mu_s, \varepsilon_s)$ ,  $s = 1, 2, \dots, M$ . In this paper, the scattering from this structure illuminated by a TM or TE plane wave with incident angle  $\varphi_0$ , is analyzed by a hybrid T-matrix and Microwave Network Approach. The formulation details are discussed in following sections.

## 3. MICROWAVE NETWORK APPROACH FOR T-MATRIX OF SINGLE CHANNEL

First, let us only consider the one channel problem as shown in Fig. 1(b). A local coordinate system is set up at the cylinder center. In this local coordinates, the incident wave could be expressed as [3]:

$$\phi_z^{inc} = \begin{cases} \sum_{n=1}^{\infty} a_n J_n(k_a \rho) \sin n\varphi & \text{TM case} \\ \sum_{n=0}^{\infty} a_n J_n(k_a \rho) \cos n\varphi & \text{TE case} \end{cases} \quad \varphi \in [0, \pi] \quad (1)$$

and the scattering (diffraction) field could be expanded as (time-harmonic factor  $e^{j\omega t}$  is assumed and suppressed throughout the paper):

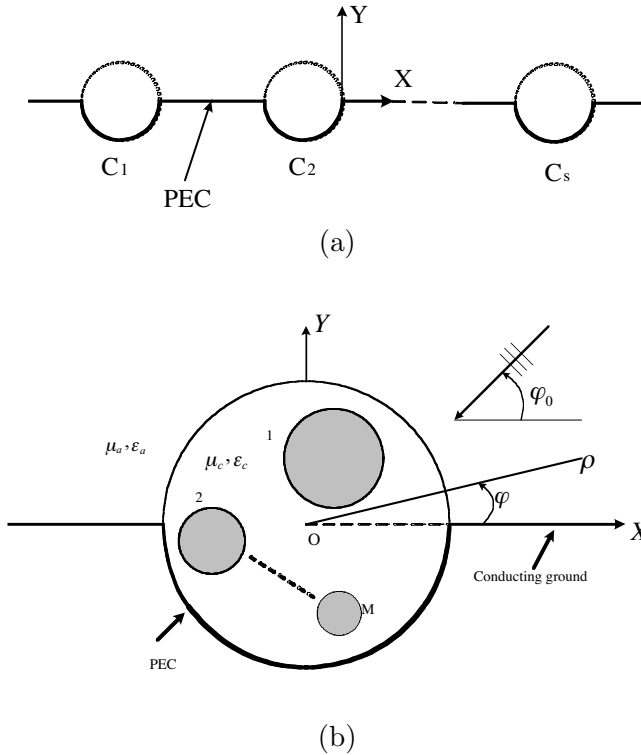


**Figure 1.** (a) Schematic illustration of parallel semicircular channels in a perfect electric conducting ground. (b) Geometric structure of a single channel as an example.

$$\phi_z^s = \begin{cases} \sum_{n=1}^{\infty} b_n H_n^{(2)}(k_a \rho) \sin n\varphi & \text{TM case} \\ \sum_{n=0}^{\infty} b_n H_n^{(2)}(k_a \rho) \cos n\varphi & \text{TE case} \end{cases} \quad \varphi \in [0, \pi] \quad (2)$$

in (1) and (2),  $J_n(\cdot)$  and  $H_n^{(2)}(\cdot)$  are Bessel functions and second kind Hankel functions, and  $\phi_z = E_z$  for TM case,  $\phi_z = H_z$  for TE case, respectively.

In this section, a linear relation between the expansion coefficient vectors  $\mathbf{b} = \{b_n\}$  and  $\mathbf{a} = \{a_n\}$  will be derived as  $\mathbf{b} = \mathbf{T}\mathbf{a}$ . The matrix  $\mathbf{T}$  is called transition matrix or T-matrix. To derive the T-matrix of a complex semicircular channel like Fig. 1(b), an equivalent microwave

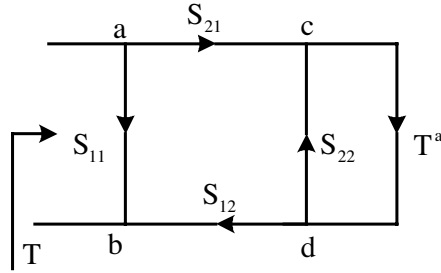


**Figure 2.** The equivalent microwave network for T-matrix of a single channel with multiple cylindrical inclusions.

network is first proposed as shown in Fig. 2. In this equivalent network, a two-port network with s-parameters  $\mathbf{S}_{ij}, i, j, = 1, 2$  is used to represent the reflection and penetration of modes from both side of the boundary of the semicircular channel. The loading matrix  $\mathbf{T}^a$  is supposed to describe the reflection from the inclusive cylinders.

Once the equivalent network has been set up, the transition matrix of the whole structure could be obtained steadily by:

$$\mathbf{T} = \mathbf{S}_{11} + \mathbf{S}_{12}\mathbf{T}^a(\mathbf{I} - \mathbf{S}_{22}\mathbf{T}^a)^{-1}\mathbf{S}_{21} \quad (3)$$

Equation (3) is quite general. For a channel with no inclusions as in [3, 4], the loading matrix  $\mathbf{T}^a$  will be vanished. On the other hand, for a channel loaded by a coaxial cylinder as in [5], the loading matrix  $\mathbf{T}^a$  will be the well known T-matrix of the circular dielectric cylinder. Therefore, the microwave network provides a powerful and flexible approach for analysis of semicircular channels. Following subsections will describe the meaning and calculation of the network parameters in details.

### 3.1. S-Parameters Description of Semicircular Boundary

The boundary condition of electromagnetic field on the channel interface  $\rho = a$ , i.e., continuity of tangential electric and magnetic field, leads to following equations:

$$E_z^{int} = \begin{cases} E_z^{out} & \varphi \in [0, \pi] \\ 0 & \varphi \in [\pi, 2\pi] \end{cases} \quad (4)$$

$$\frac{1}{\mu_c}\partial_\rho E_z^{int} = \frac{1}{\mu_a}\partial_\rho E_z^{out} \quad \varphi \in [0, \pi] \quad (5)$$

for the TM wave incidence, and

$$H_z^{int} = H_z^{out} \quad \varphi \in [0, \pi] \quad (6)$$

$$\frac{1}{\varepsilon_c} \partial_\rho H_z^{int} = \begin{cases} \frac{1}{\varepsilon_a} \partial_\rho H_z^{out} & \varphi \in [0, \pi] \\ 0 & \varphi \in [\pi, 2\pi] \end{cases} \quad (7)$$

for the TE wave incidence. For the simplicity, the formulas for TM wave are derived in detail while only final formulas are listed for TE wave. When a TM wave illuminates the semicircular channel, the external and internal electric field could be expressed as

$$E_z^{out} = \sum_{n=1}^{\infty} \left[ a_n J_n(k_a \rho) \sin(n\varphi) + b_n H_n^{(2)}(k_a \rho) \sin(n\varphi) \right] \quad \rho \geq a, \varphi \in [0, \pi] \quad (8)$$

$$E_z^{int} = \sum_{n=-\infty}^{\infty} \left[ c_n J_n(k_c \rho) e^{jn\varphi} + d_n H_n^{(2)}(k_c \rho) e^{jn\varphi} \right] \quad \rho \leq a, \varphi \in [0, 2\pi] \quad (9)$$

where  $k_s = k_0 \sqrt{\mu_s \varepsilon_s}$ ,  $s = a, c$  is the wave number of the medium. Substituting (8), (9) into (4) and (5), we have:

$$\begin{aligned} & \sum_{n=-Q}^Q \left[ c_n J_n(k_c a) e^{jn\varphi} + d_n H_n^{(2)}(k_c a) e^{jn\varphi} \right] \\ = & \begin{cases} \sum_{n=1}^N \left[ a_n J_n(k_a a) \sin(n\varphi) + b_n H_n^{(2)}(k_a a) \sin(n\varphi) \right] & \varphi \in [0, \pi] \\ 0 & \varphi \in [\pi, 2\pi] \end{cases} \end{aligned} \quad (10)$$

$$\begin{aligned} & \sum_{n=-Q}^Q \left[ c_n \eta_c^{-1} J_n'(k_c a) e^{jn\varphi} + d_n \eta_c^{-1} H_n^{(2)'}(k_c a) e^{jn\varphi} \right] \\ = & \sum_{n=1}^N \left[ a_n \eta_a^{-1} J_n'(k_a a) \sin(n\varphi) + b_n \eta_a^{-1} H_n^{(2)'}(k_a a) \sin(n\varphi) \right] \varphi \in [0, \pi] \end{aligned} \quad (11)$$

where  $\eta_s = \sqrt{\mu_s / \varepsilon_s}$ ,  $s = a, c$  stands for the wave impedance of the medium. Notice that the finite number of cylindrical harmonics or

modes is used in Equation (10) and (11), i.e., we use  $2Q + 1$  and  $N$  modes to approximate the internal and external fields respectively.

Multiplying both side of Equation (10) with the function  $e^{-jm\varphi}$ ,  $m \in Z$ , and  $m \in [-Q, Q]$  and integrating the angle  $\varphi$  from 0 to  $2\pi$ , then we have:

$$\mathbf{J}_c \mathbf{c} + \mathbf{H}_c \mathbf{d} = \mathbf{J}_a \mathbf{a} + \mathbf{H}_a \mathbf{b} \quad (12)$$

where  $\mathbf{a}$ ,  $\mathbf{b}$ ,  $\mathbf{c}$ ,  $\mathbf{d}$  are vectors denoting corresponding expansion coefficients and  $\mathbf{J}_c$ ,  $\mathbf{H}_c$  are  $(2Q + 1) \times (2Q + 1)$  matrices and  $\mathbf{J}_a$ ,  $\mathbf{H}_a$ ,  $(2Q + 1) \times N$  matrices, whose elements could be evaluated as:

$$\mathbf{J}_c(m, n) = 2\pi J_n(k_c a) \delta_{nm} \quad -Q \leq n, m \leq Q \quad (13a)$$

$$\mathbf{H}_c(m, n) = 2\pi H_n^{(2)}(k_c a) \delta_{nm} \quad -Q \leq n, m \leq Q \quad (13b)$$

$$\mathbf{J}_a(m, n) = J_n(k_a a) f(n, m) \quad -Q \leq m \leq Q, 1 \leq n \leq N \quad (13c)$$

$$\mathbf{H}_a(m, n) = H_n^{(2)}(k_a a) f(n, m) \quad -Q \leq m \leq Q, 1 \leq n \leq N \quad (13d)$$

Similarly, multiplying both sides of Equation (11) with function  $\sin m\varphi$ ,  $m = 1, 2, \dots, N$  and integrating the angle  $\varphi$  from 0 to  $\pi$ , then results in following equations:

$$\mathbf{J}'_c \mathbf{c} + \mathbf{H}'_c \mathbf{d} = \mathbf{J}'_a \mathbf{a} + \mathbf{H}'_a \mathbf{b} \quad (14)$$

where  $\mathbf{J}'_c$ ,  $\mathbf{H}'_c$  are  $N \times (2Q + 1)$  matrices and  $\mathbf{J}'_a$ ,  $\mathbf{H}'_a$  are  $N \times N$  matrices, which could be obtained by:

$$\mathbf{J}'_c(m, n) = \eta_c^{-1} J'_n(k_c a) f(m, -n) \quad -Q \leq n \leq Q, 1 \leq m \leq N \quad (15a)$$

$$\mathbf{H}'_c(m, n) = \eta_c^{-1} H_n^{(2)'}(k_c a) f(m, -n) \quad -Q \leq n \leq Q, 1 \leq m \leq N \quad (15b)$$

$$\mathbf{J}'_a(m, n) = \frac{\pi}{2} \eta_a^{-1} J'_n(k_a a) \delta_{mn} \quad 1 \leq n \leq N, 1 \leq m \leq N \quad (15c)$$

$$\mathbf{H}'_a(m, n) = \frac{\pi}{2} \eta_a^{-1} H_n^{(2)'}(k_a a) \delta_{mn} \quad 1 \leq n \leq N, 1 \leq m \leq N \quad (15d)$$

where  $\delta_{mn}$  is the Kronecker's delta; and the function  $f(m, n)$  in (13c), (13d) and (15c), (15b) is defined as:

$$f(m, n) = \int_0^\pi \sin m\varphi e^{-jn\varphi} d\varphi$$

$$= \begin{cases} +\frac{\pi}{2j} & m = n \\ -\frac{\pi}{2j} & m = -n \\ \frac{1}{2} \left[ \frac{1 - \cos(m+n)\pi}{m+n} + \frac{1 - \cos(m-n)\pi}{m-n} \right] & m \neq \pm n \end{cases} \quad (16)$$

Combining Equation (12) and (14), we have:

$$\begin{bmatrix} \mathbf{H}_a & -\mathbf{J}_c \\ \mathbf{H}'_a & -\mathbf{J}'_c \end{bmatrix} \begin{bmatrix} b \\ c \end{bmatrix} = \begin{bmatrix} -\mathbf{J}_a & \mathbf{H}_c \\ -\mathbf{J}'_a & \mathbf{H}'_c \end{bmatrix} \begin{bmatrix} a \\ d \end{bmatrix} \quad (17)$$

Then s-parameters could be obtained by:

$$\begin{bmatrix} \mathbf{S}_{11} & \mathbf{S}_{12} \\ \mathbf{S}_{21} & \mathbf{S}_{122} \end{bmatrix} = \begin{bmatrix} \mathbf{H}_a & -\mathbf{J}_c \\ \mathbf{H}'_a & -\mathbf{J}'_c \end{bmatrix}^{-1} \begin{bmatrix} -\mathbf{J}_a & \mathbf{H}_c \\ -\mathbf{J}'_a & \mathbf{H}'_c \end{bmatrix} \quad (18)$$

Explicit expressions for s-parameter matrices could be derived as:

$$\mathbf{S}_{11} = \left( \mathbf{H}'_a - \mathbf{J}'_c \mathbf{J}_c^{-1} \mathbf{H}_a \right)^{-1} \left( \mathbf{J}'_c \mathbf{J}_c^{-1} \mathbf{J}_a - \mathbf{J}'_a \right) \quad (19a)$$

$$\mathbf{S}_{21} = \mathbf{J}_c^{-1} \left( \mathbf{H}_a \mathbf{S}_{11} + \mathbf{J}_a \right) \quad (19b)$$

$$\mathbf{S}_{22} = \left( \mathbf{H}_a \mathbf{H}'_a^{-1} \mathbf{J}'_c - \mathbf{J}_c \right)^{-1} \left( \mathbf{H}_c - \mathbf{H}_a \mathbf{H}'_a^{-1} \mathbf{H}'_c \right) \quad (19c)$$

$$\mathbf{S}_{12} = \mathbf{H}'_a^{-1} \left( \mathbf{J}'_c \mathbf{S}_{22} + \mathbf{H}'_c \right) \quad (19d)$$

where the sub-matrices  $\mathbf{S}_{11}, \mathbf{S}_{12}, \mathbf{S}_{21}, \mathbf{S}_{22}$  are, respectively,  $N \times N$ ,  $N \times (2Q+1)$ ,  $(2Q+1) \times N$ ,  $(2Q+1) \times (2Q+1)$ , matrices. Therefore, we have derived an explicit formula for the s-parameters of semicircular channels for the TM wave. In a similar way, we can obtain the following formulas for the TE wave:

$$\mathbf{S}_{11} = \left( \mathbf{H}_a - \mathbf{J}_c \mathbf{J}'_c^{-1} \mathbf{H}'_a \right)^{-1} \left( \mathbf{J}_c \mathbf{J}'_c^{-1} \mathbf{J}'_a - \mathbf{J}_a \right) \quad (20a)$$

$$\mathbf{S}_{21} = \mathbf{J}'_c^{-1} \left( \mathbf{H}'_a \mathbf{S}_{11} + \mathbf{J}'_a \right) \quad (20b)$$

$$\mathbf{S}_{22} = \left( \mathbf{H}'_a \mathbf{H}_a^{-1} \mathbf{J}_c - \mathbf{J}'_c \right)^{-1} \left( \mathbf{H}'_c - \mathbf{H}'_a \mathbf{H}_a^{-1} \mathbf{H}_c \right) \quad (20c)$$

$$\mathbf{S}_{12} = \mathbf{H}_a^{-1} \left( \mathbf{J}_c \mathbf{S}_{22} + \mathbf{H}_c \right) \quad (20d)$$

The elements of matrices in (20b)–(20d) could be evaluated as:

$$\mathbf{J}_c(m, n) = J_n(k_a a) g(-n, m) \quad 0 \leq m \leq N, -Q \leq n \leq Q \quad (21a)$$

$$\mathbf{H}_c(m, n) = H_n^{(2)}(k_c a) g(-n, m) \quad 0 \leq m \leq N, -Q \leq n \leq Q \quad (21b)$$

$$\mathbf{J}_a(m, n) = J_n(k_a a) h(m, n) \quad 0 \leq m, n \leq N \quad (21c)$$

$$\mathbf{H}_a(m, n) = H_n^{(2)}(k_a a) h(m, n) \quad 0 \leq m, n \leq N \quad (21d)$$

$$\mathbf{J}'_c(m, n) = 2\pi\eta_c J'_n(k_c a) \delta_{mn} \quad -Q \leq m, n \leq Q \quad (21e)$$

$$\mathbf{H}'_c(m, n) = 2\pi\eta_c H_n^{(2)'}(k_c a) \delta_{mn} \quad -Q \leq m, n \leq Q \quad (21f)$$

$$\mathbf{J}'_a(m, n) = \frac{\pi}{2} \eta_a J'_n(k_a a) g(m, n) \quad -Q \leq m \leq Q, 0 \leq n \leq N \quad (21g)$$

$$\mathbf{H}'_a(m, n) = \frac{\pi}{2} \eta_a H_n^{(2)'}(k_a a) g(m, n) \quad -Q \leq m \leq Q, 0 \leq n \leq N \quad (21h)$$



where the functions  $g(m, n)$ ,  $h(m, n)$  are defined as:

$$g(m, n) = \int_0^\pi e^{-jm\varphi} \cos n\varphi d\varphi$$

$$= \begin{cases} \pi & m = n = 0 \\ \frac{\pi}{2} & m = \pm n \neq 0 \\ -\frac{j}{2} \left[ \frac{1 - \cos(m+n)\pi}{m+n} + \frac{1 - \cos(m-n)\pi}{m-n} \right] & m \neq \pm n \neq 0 \end{cases} \quad (22)$$

$$h(m, n) = \int_0^\pi \cos m\varphi \cos n\varphi d\varphi = \begin{cases} \pi & m = n = 0 \\ \frac{\pi}{2} & m = \pm n \neq 0 \\ 0 & m \neq \pm n \neq 0 \end{cases} \quad (23)$$

Thus, both TM and TE s-parameter matrices for a single semicircular channel have been obtained.

### 3.2. Aggregated T-Matrix of Multiple Circular Cylinders

Fig. 3 illustrates the geometry of multiple parallel circular cylinders. Scattering from parallel cylinders has been investigated by many authors. However, we will give a new approach which could obtain the T-matrix of multiple cylinders directly from the T-matrix of the inclusive cylinders using the addition theorems of cylindrical harmonics.

A fictitious circular cylinder is assumed to enclose all the inclusive cylinders. The scattering property of this fictitious circular cylinder could be described by its transition-matrix denoted as  $\mathbf{T}^a$ . Assuming the incident wave upon multiple cylinders is written

$$\phi^{inc} = \sum_{n=-\infty}^{\infty} a_{0n} J_n(k_c \rho) e^{jn\varphi} \quad (24)$$

and the scattering field outside the fictitious cylinder is expressed as

$$\phi^s = \sum_{n=-\infty}^{\infty} f_{0n} H_n^{(2)}(k_c \rho) e^{jn\varphi} \quad (25)$$

so the problem becomes to derive a formula to relate outward coefficient vector  $\mathbf{f}_0$  with inward coefficient vector  $\mathbf{a}_0$  as  $\mathbf{f}_0 = \mathbf{T}^a \mathbf{a}_0$ . To do so, the

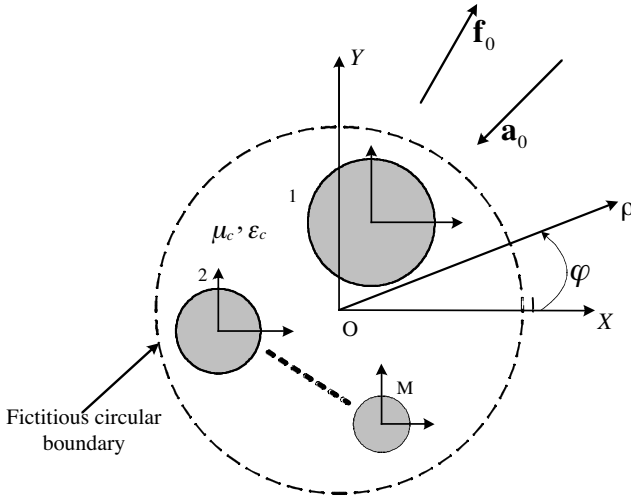


**Figure 3.** Multiple circular cylinders and the fictitious circular boundary.

field outside the fictitious boundary is viewed in another way as the superposition of scattering field from each inclusive cylinder in its local coordinate system and could be expressed as:

$$\phi^s = \sum_{i=1}^M \sum_{n=-\infty}^{\infty} f_{in} H_n^{(2)}(k_c |\boldsymbol{\rho} - \boldsymbol{\rho}_i|) e^{jn \arg(\boldsymbol{\rho} - \boldsymbol{\rho}_i)} \quad (26)$$

where  $\boldsymbol{\rho}$  is the observation point and  $\boldsymbol{\rho}_i$  is the center of  $i$ th inclusive cylinder. The coefficients for the outward wave in local coordinates of each cylinder satisfy following equation:

$$\mathbf{f}_i = \mathbf{T}_i \left( \beta_{i0} \mathbf{a}_0 + \sum_{\substack{j=1 \\ j \neq i}}^M \alpha_{ij} \mathbf{f}_j \right) \quad i = 1, 2, \dots, N \quad (27)$$

In (27),  $\mathbf{a}_0$  stands for the expansion coefficient vector of the incident wave in main coordinates;  $\mathbf{T}_i$  denotes the T-matrix of  $i$ th cylinder; the matrices  $\beta_{i0}$  and  $\alpha_{ij}$  are the transform matrices of cylindrical harmonics between different coordinate systems and their calculations are obtained by the addition theorems of cylindrical harmonics. The addition theorems of cylindrical harmonics have been well described in [12] and [13]. The physical meaning of Equation (27) could be explained as that for  $i$ th cylinder, the incident wave comes from two

parts: One from the incident wave outside the fictitious boundary; another from the scattering field of other cylinders.

Furthermore, the outward field  $\mathbf{f}_0$  in main frame is the summation of  $\mathbf{f}_i$  in its local frame and we have following equation using the addition theorem of cylindrical harmonics:

$$\mathbf{f}_0 = \sum_{i=1}^M \beta_{0i} \mathbf{f}_i \quad (28)$$

Equation (27) and (28) lead to

$$\mathbf{T}^a = \beta_{0M} \left( \mathbf{I} - \mathbf{T}^{(M)} \boldsymbol{\alpha} \right)^{-1} \mathbf{T}^{(M)} \beta_{M0}^T \quad (29)$$

where  $\mathbf{I}$  denotes a unit matrix;  $\mathbf{T}^{(M)}$  stands for T-matrix of inclusive circular cylinders and could be expressed as:

$$\mathbf{T}^{(M)} = \begin{bmatrix} \mathbf{T}_1 & 0 & \cdots & 0 \\ 0 & \mathbf{T}_2 & \cdots & 0 \\ \vdots & \vdots & \ddots & \vdots \\ 0 & 0 & \cdots & \mathbf{T}_M \end{bmatrix} \quad (30)$$

the matrix  $\boldsymbol{\alpha}$  in (29) represents the mutual interactions among cylinders and is defined as:

$$\boldsymbol{\alpha} = \begin{bmatrix} 0 & \alpha_{12} & \cdots & \alpha_{1M} \\ \alpha_{21} & 0 & \cdots & \alpha_{2M} \\ \vdots & \vdots & \ddots & \vdots \\ \alpha_{M1} & \alpha_{M2} & \cdots & 0 \end{bmatrix} \quad (31)$$

In (29), the matrices  $\beta_{0M}$  and  $\beta_{M0}^T$  represent the wave transform between cylinder centers and the origin point of the fictitious circular cylinder and could be obtained by following formula:

$$\beta_{0M} = [\beta_{01} \ \beta_{02} \ \cdots \ \beta_{0M}] \quad (32)$$

$$\beta_{M0}^T = [\beta_{10} \ \beta_{20} \ \cdots \ \beta_{M0}]^T \quad (33)$$

where symbol  $T$  in (33) denotes the transpose of the matrix. For the completeness, the T-matrix of circular cylinders is listed below:

$$\mathbf{T}(m, n) = -\frac{J_n(k_1 a)}{H_n^{(2)}(k_1 a)} \delta_{mn} \quad \text{TM case} \quad (34)$$

$$\mathbf{T}(m, n) = -\frac{J'_n(k_1 a)}{H_n^{(2)'}(k_1 a)} \delta_{mn} \quad \text{TE case} \quad (35)$$

for metal cylinders and

$$\mathbf{T}(m, n) = \frac{\eta_1 J_n(k_1 a) J_n'(k_2 a) - \eta_2 J_n'(k_1 a) J_n(k_2 a)}{\eta_2 J_n(k_2 a) H_n^{(2)'}(k_1 a) - \eta_1 J_n'(k_2 a) H_n^{(2)}(k_1 a)} \delta_{mn} \quad \text{TM case} \quad (36)$$

$$\mathbf{T}(m, n) = \frac{\eta_2 J_n(k_1 a) J_n'(k_2 a) - \eta_1 J_n'(k_1 a) J_n(k_2 a)}{\eta_1 J_n(k_2 a) H_n^{(2)'}(k_1 a) - \eta_2 J_n'(k_2 a) H_n^{(2)}(k_1 a)} \delta_{mn} \quad \text{TE case} \quad (37)$$

for dielectric cylinders and  $\eta_i = \sqrt{\mu_i/\varepsilon_i}$ ,  $i = 1, 2$  is the wave impedance of the dielectrics.

#### 4. T-MATRIX APPROACH FOR MULTIPLE SCATTERING FROM PARALLEL CHANNELS

To consider the multiple scattering between parallel channels using the T-matrix derived above, a new set of addition theorems in half space instead of those in free space given in Appendix D of [14] should be derived. Although the authors in [8] have already utilized the addition theorems in half space, they did not give them in an explicit form. To facilitate our discussion, addition theorems in half space are derived and listed as follows:

$$H_m^{(2)}(k|\boldsymbol{\rho} - \boldsymbol{\rho}_j|) \cos m\varphi_j = \begin{cases} \sum_{n=0}^{\infty} \frac{2 - \delta_{n0}}{2} \left\{ \begin{array}{l} [J_{n-m}(k\rho_{ji}) + (-1)^m J_{n+m}(k\rho_{ji})] \\ \cos n\varphi_{ji} \cos m\varphi_{ji} \end{array} \right\} \\ \quad \times H_n^{(2)}(k|\boldsymbol{\rho} - \boldsymbol{\rho}_i|) \cos n\varphi_i \quad |\boldsymbol{\rho} - \boldsymbol{\rho}_i| > \rho_{ji} \\ \sum_{n=0}^{\infty} \frac{2 - \delta_{n0}}{2} \left\{ \begin{array}{l} [H_{n-m}^{(2)}(k\rho_{ji}) + (-1)^m H_{n+m}^{(2)}(k\rho_{ji})] \\ \cos n\varphi_{ji} \cos m\varphi_{ji} \end{array} \right\} \\ \quad \times J_n(k|\boldsymbol{\rho} - \boldsymbol{\rho}_i|) \cos n\varphi_i \quad |\boldsymbol{\rho} - \boldsymbol{\rho}_i| < \rho_{ji} \end{cases} \quad (38)$$

$$J_m(k|\boldsymbol{\rho} - \boldsymbol{\rho}_j|) \cos m\varphi_j = \sum_{n=0}^{\infty} \frac{2 - \delta_{n0}}{2} \left\{ \begin{array}{l} J_{n-m}(k\rho_{ji}) + (-1)^m J_{n+m}(k\rho_{ji}) \\ \cos n\varphi_{ji} \cos m\varphi_{ji} \end{array} \right\} \\ \quad \times J_n(k|\boldsymbol{\rho} - \boldsymbol{\rho}_i|) \cos n\varphi_i \quad (39)$$

$$\begin{aligned}
 & H_m^{(2)}(k|\boldsymbol{\rho} - \boldsymbol{\rho}_j|) \sin m\varphi_j \\
 &= \begin{cases} \sum_{n=1}^{\infty} \left\{ \begin{aligned} & [J_{n-m}(k\rho_{ji}) - (-1)^m J_{n+m}(k\rho_{ji})] \\ & \cos n\varphi_{ji} \cos m\varphi_{ji} \\ & \times H_n^{(2)}(k|\boldsymbol{\rho} - \boldsymbol{\rho}_i|) \sin n\varphi_i \quad |\boldsymbol{\rho} - \boldsymbol{\rho}_i| > \rho_{ji} \end{aligned} \right\} \\ \\ \sum_{n=1}^{\infty} \left\{ \begin{aligned} & [H_{n-m}^{(2)}(k\rho_{ji}) - (-1)^m H_{n+m}^{(2)}(k\rho_{ji})] \\ & \cos n\varphi_{ji} \cos m\varphi_{ji} \\ & \times J_n(k|\boldsymbol{\rho} - \boldsymbol{\rho}_i|) \sin n\varphi_i \quad |\boldsymbol{\rho} - \boldsymbol{\rho}_i| < \rho_{ji} \end{aligned} \right\} \end{cases} \quad (40)
 \end{aligned}$$

$$\begin{aligned}
 & J_m(k|\boldsymbol{\rho} - \boldsymbol{\rho}_j|) \sin m\varphi_j \\
 &= \sum_{n=1}^{\infty} \left\{ \begin{aligned} & [J_{n-m}(k\rho_{ji}) - (-1)^m J_{n+m}(k\rho_{ji})] \\ & \cos n\varphi_{ji} \cos m\varphi_{ji} \\ & \times J_n(k|\boldsymbol{\rho} - \boldsymbol{\rho}_i|) \sin n\varphi_i \end{aligned} \right\} \quad (41)
 \end{aligned}$$

Equ. (38) and (39) are used for TE case while Equation (40) and (41) are utilized for TM case. The geometric meaning of the parameters in (38)–(41) is shown in Fig. 4. It is worth to emphasize that  $\varphi_{ji} = \arg(\boldsymbol{\rho}_j - \boldsymbol{\rho}_i)$ , which means if  $\boldsymbol{\rho}_j$  lies on the right of  $\boldsymbol{\rho}_i$ , then  $\varphi_{ji} = 0$  while  $\boldsymbol{\rho}_j$  lies on the left of  $\boldsymbol{\rho}_i$ ,  $\varphi_{ji} = \pi$ .

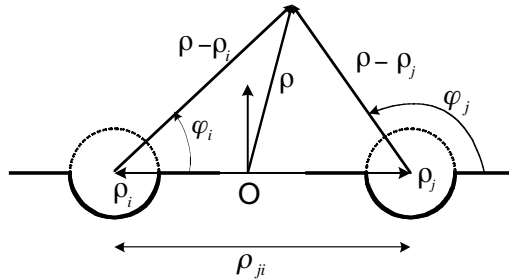


**Figure 4.** Coordinate systems in two semicircular channels.

Then following the same procedure described in Section 3.2, we have:

$$\mathbf{f}_i^c = \mathbf{T}_i^C \left( \boldsymbol{\beta}_{i0}^C \mathbf{a}_0 + \sum_{\substack{j=1 \\ j \neq i}}^{N_C} \boldsymbol{\alpha}_{ij}^C \mathbf{f}_j^c \right) \quad i = 1, 2, \dots, N_C \quad (42)$$

where  $\mathbf{f}_i^c$  and  $\mathbf{T}_i^C$  stand for the expansion coefficients of scattering wave from the  $i$ -th channel and its T-matrix in its local coordinates;  $\boldsymbol{\beta}_{i0}^C$  and

$\alpha_{ij}^C$  are wave transform matrices obtained from addition theorem (34)–(37). Their elements are:

$$\beta_{i0}^C(m, n) = \begin{cases} \begin{bmatrix} J_{m-n}(k_a \rho_i)^- \\ (-1)^n J_{m+n}(k_a \rho_i) \end{bmatrix} \cos n \varphi_{ji} \cos m \varphi_{ji} & m, n = 1, 2, \dots \text{ TM case} \\ \frac{2 - \delta_{m0}}{2} \begin{bmatrix} J_{m-n}(k_a \rho_i)^+ \\ (-1)^n J_{m+n}(k_a \rho_i) \end{bmatrix} \cos n \varphi_{ji} \cos m \varphi_{ji} & m, n = 0, 2, \dots \text{ TE case} \end{cases} \quad (43)$$

and

$$\alpha_{ij}^C(m, n) = \begin{cases} \begin{bmatrix} H_{m-n}^{(2)}(k_c \rho_{ij})^- \\ (-1)^n H_{m+n}^{(2)}(k_c \rho_{ij}) \end{bmatrix} \cos n \varphi_{ji} \cos m \varphi_{ji} & m, n = 1, 2, \dots \text{ TM case} \\ \frac{2 - \delta_{m0}}{2} \begin{bmatrix} H_{m-n}^{(2)}(k_c \rho_{ij})^+ \\ (-1)^n H_{m+n}^{(2)}(k_c \rho_{ij}) \end{bmatrix} \cos n \varphi_{ji} \cos m \varphi_{ji} & m, n = 0, 1, \dots \text{ TE case} \end{cases} \quad (44)$$

There are two approaches to solve Equation (42). The first one is using iterative solution as in [15]. One iteration represents one time of mutual interactions among all channels. After several iterations,  $\mathbf{f}_i^C$  would converge to a stable value. Another solution is to invert the final matrix as follows:

$$\begin{bmatrix} \mathbf{f}_1^C \\ \mathbf{f}_2^C \\ \vdots \\ \mathbf{f}_{N_C}^C \end{bmatrix} = \left\{ \mathbf{I} - \begin{bmatrix} \mathbf{T}_1^C & 0 & \cdots & 0 \\ 0 & \mathbf{T}_2^C & \cdots & 0 \\ \vdots & \vdots & \ddots & \vdots \\ 0 & 0 & \cdots & \mathbf{T}_{N_C}^C \end{bmatrix} \begin{bmatrix} 0 & \alpha_{12}^C & \cdots & \alpha_{1N_C}^C \\ \alpha_{21}^C & 0 & \cdots & \alpha_{2N_C}^C \\ \vdots & \vdots & \ddots & \vdots \\ \alpha_{N_C1}^C & \alpha_{N_C2}^C & \cdots & 0 \end{bmatrix} \right\}^{-1}$$

$$\times \begin{bmatrix} \mathbf{T}_1^C & 0 & \cdots & 0 \\ 0 & \mathbf{T}_2^C & \cdots & 0 \\ \vdots & \vdots & \ddots & \vdots \\ 0 & 0 & \cdots & \mathbf{T}_{N_C}^C \end{bmatrix} \begin{bmatrix} \beta_{i0}^C \\ \beta_{i0}^C \\ \vdots \\ \beta_{i0}^C \end{bmatrix} \mathbf{a}_0 \quad (45)$$

The inverse of the matrix in (45) means infinite number of multiple scattering has been considered. Obviously, aggregated T-matrix approach could also be utilized to obtain the T-matrix of multiple channels. The T-matrix of parallel channels will greatly simplify the calculation of far field. (In this paper, we restrict us in far field computation although the near field distribution could be obtained steadily). Therefore, similar to Equation (29), we have following formula for aggregated T-matrix of parallel channels:

$$\begin{aligned} \mathbf{T}^C &= [\beta_{01}^C \ \beta_{02}^C \ \cdots \ \beta_{0N_C}^C] \\ &\left\{ \mathbf{I} - \begin{bmatrix} \mathbf{T}_1^C & 0 & \cdots & 0 \\ 0 & \mathbf{T}_2^C & \cdots & 0 \\ \vdots & \vdots & \ddots & \vdots \\ 0 & 0 & \cdots & \mathbf{T}_{N_C}^C \end{bmatrix} \begin{bmatrix} 0 & \alpha_{12}^C & \cdots & \alpha_{1N_C}^C \\ \alpha_{21}^C & 0 & \cdots & \alpha_{2N_C}^C \\ \vdots & \vdots & \ddots & \vdots \\ \alpha_{N_C1}^C & \alpha_{N_C2}^C & \cdots & 0 \end{bmatrix} \right\}^{-1} \\ &\times \begin{bmatrix} \mathbf{T}_1^C & 0 & \cdots & 0 \\ 0 & \mathbf{T}_2^C & \cdots & 0 \\ \vdots & \vdots & \ddots & \vdots \\ 0 & 0 & \cdots & \mathbf{T}_{N_C}^C \end{bmatrix} \begin{bmatrix} \beta_{i0}^C \\ \beta_{i0}^C \\ \vdots \\ \beta_{i0}^C \end{bmatrix} \quad (46) \end{aligned}$$

## 5. INCIDENT WAVE EXPANSION AND FAR FIELD CALCULATION

The T-matrix given in (46) describes the scattering characteristics of parallel channels and is independent of the incident wave. In this paper, we only consider the plane wave incidences although it is easier to extend to Gaussian beam incidence as in [16].

From Fig. 1(b), the incident TM plane wave is given by:

$$E_z^{inc} = \sum_{n=1}^{\infty} 4j^n \sin n\varphi_0 [J_n(k_a\rho) \sin n\varphi] \quad (47)$$

and for TE plane wave:

$$H_z^{inc} = \sum_{n=0}^{\infty} (4 - 2\delta_{n0}) j^n \cos n\varphi_0 [J_n(k_a\rho) \cos n\varphi] \quad (48)$$

Then we have the incident wave vector

$$\mathbf{a}(n) = \begin{cases} 4j^n \sin n\varphi_0 & n = 1, 2, \dots, \text{ TM case} \\ (4 - 2\delta_{n0})j^n \cos n\varphi_0 & n = 0, 1, \dots, \text{ TE case} \end{cases} \quad (49)$$

Using the Equation (46), the expansion coefficients of the scattering wave could be obtained easily by:

$$\mathbf{f} = \mathbf{T}^C \mathbf{a} \quad (50)$$

For TM wave incidence, the far field could be expressed as:

$$E_z^s = \sum_{n=1}^{\infty} f(n) [H_n^{(2)}(k_a\rho) \sin n\varphi] \quad (51)$$

for TE wave incidence, it becomes

$$H_z^s = \sum_{n=0}^{\infty} f(n) [H_n^{(2)}(k_a\rho) \cos n\varphi] \quad (52)$$

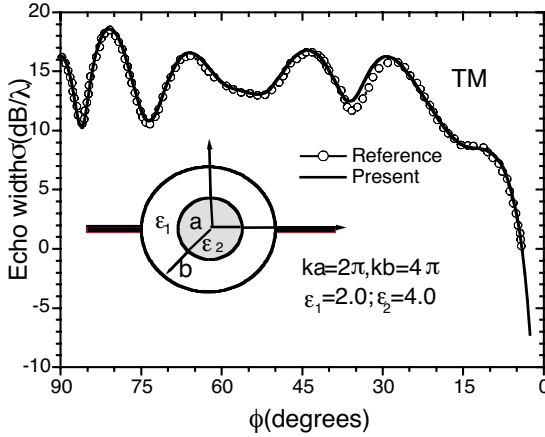
Using the large argument approximation of the Hankel functions, the echo width of parallel channel could be obtained as:

$$\sigma(\varphi) = \begin{cases} \frac{4}{k} \left| \sum_{n=1}^{\infty} f(n) j^n \sin n\varphi \right|^2 & \text{ TM case} \\ \frac{4}{k} \left| \sum_{n=0}^{\infty} f(n) j^n \cos n\varphi \right|^2 & \text{ TE case} \end{cases} \quad (53)$$

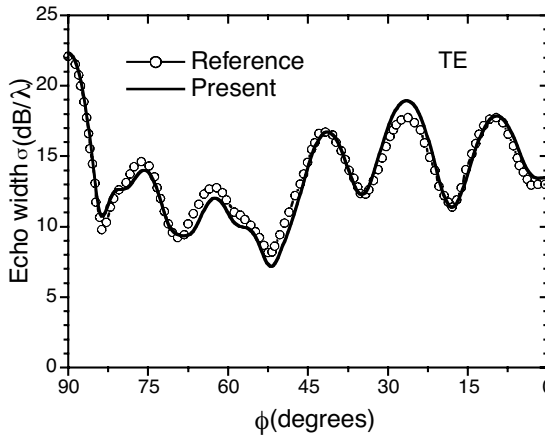
To facilitate our comparison with other authors, we also define another parameter as:

$$G(\varphi) = \begin{cases} \sum_{n=1}^{\infty} f(n) j^n \sin n\varphi & \text{ TM case} \\ \sum_{n=0}^{\infty} f(n) j^n \cos n\varphi & \text{ TE case} \end{cases} \quad (54)$$





(a)



(b)

**Figure 5.** Comparison of the present method with dual-series solution [5] for backscattering echo width from a coaxial cylinder loading semicircular channel.

## 6. CASE NUMERICAL EXAMPLES AND DISCUSSIONS

To validate the algorithm discussed above, several numerical examples are provided. Fig. 5 compares our results with an exact dual-series eigenfunctions solution [5] for backscattering echo width from a coaxial cylinder loading semicircular channel. Obviously, two methods agree very well in TM case. The difference for TE case between our results

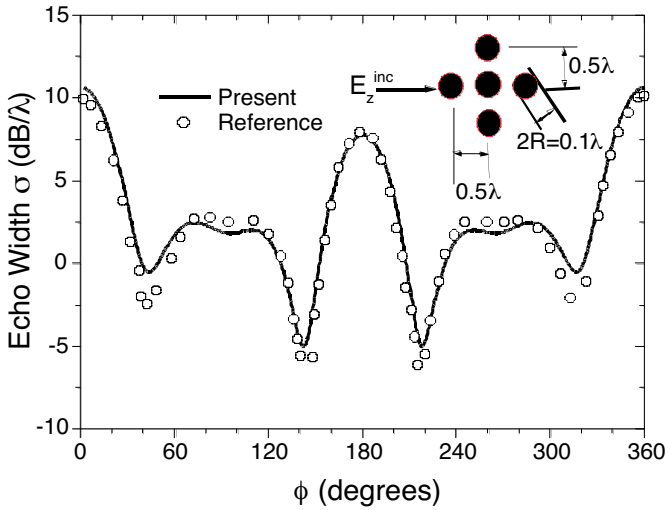


**Figure 6.** Comparison of scattering from five perfect conducting cylinders obtained by aggregated T-matrix method and iterative solution in [15].

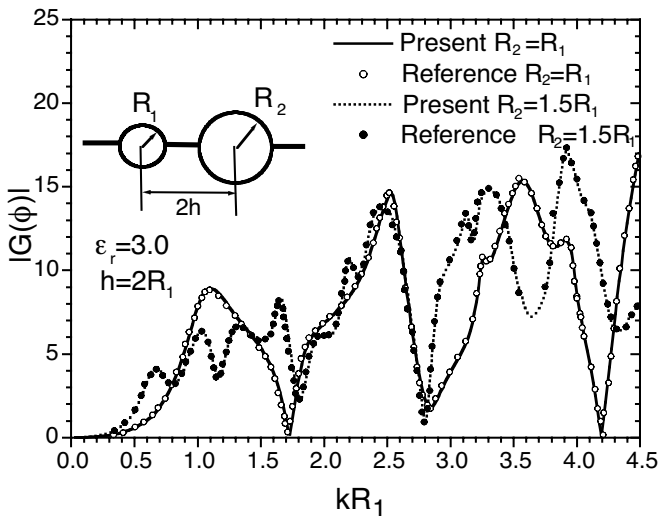


**Figure 7.** Comparison of present method and reference [8] for numerical backscattering versus  $kR_1$  from two dielectric filled semicircular channels.

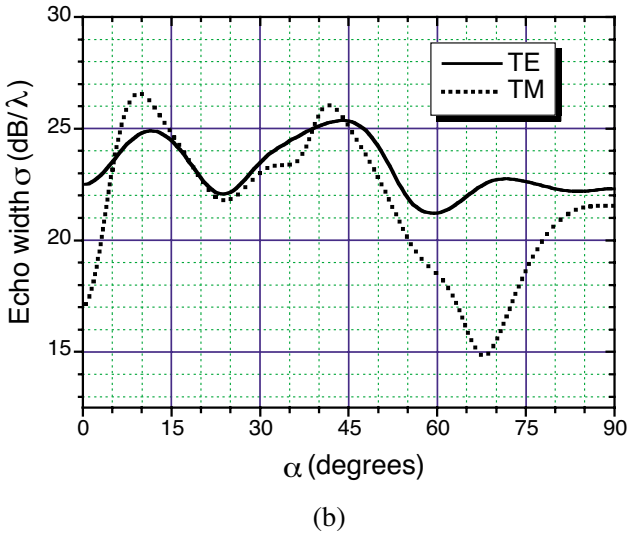
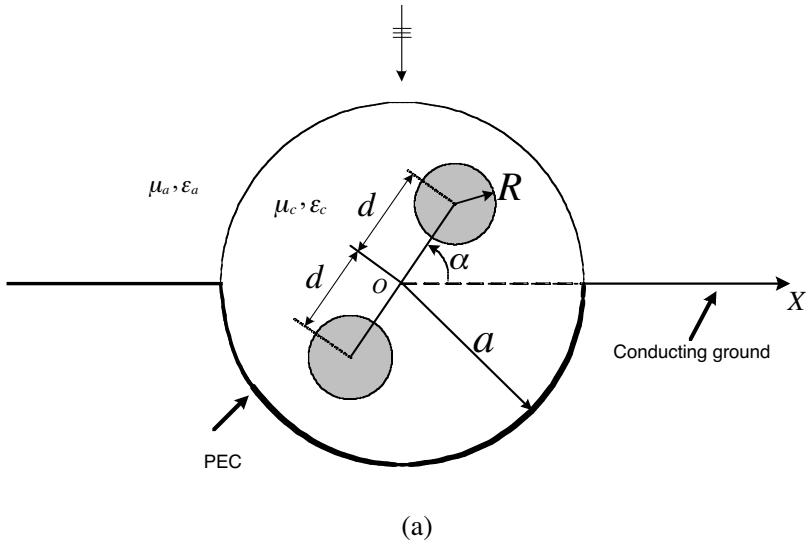


**Figure 8.** (a) A semicircular channel with two conducting cylindrical inclusions  $(\mu_a, \epsilon_a) = (1.0, 1.0)$ ,  $(\mu_c, \epsilon_c) = (1.0, 2.0)$ ,  $a = 1.5\lambda$ ,  $d = 0.9\lambda$ ,  $R = 0.2\lambda$ , (b) Backscattering versus angle  $\alpha$  for TM and TE wave incidences.

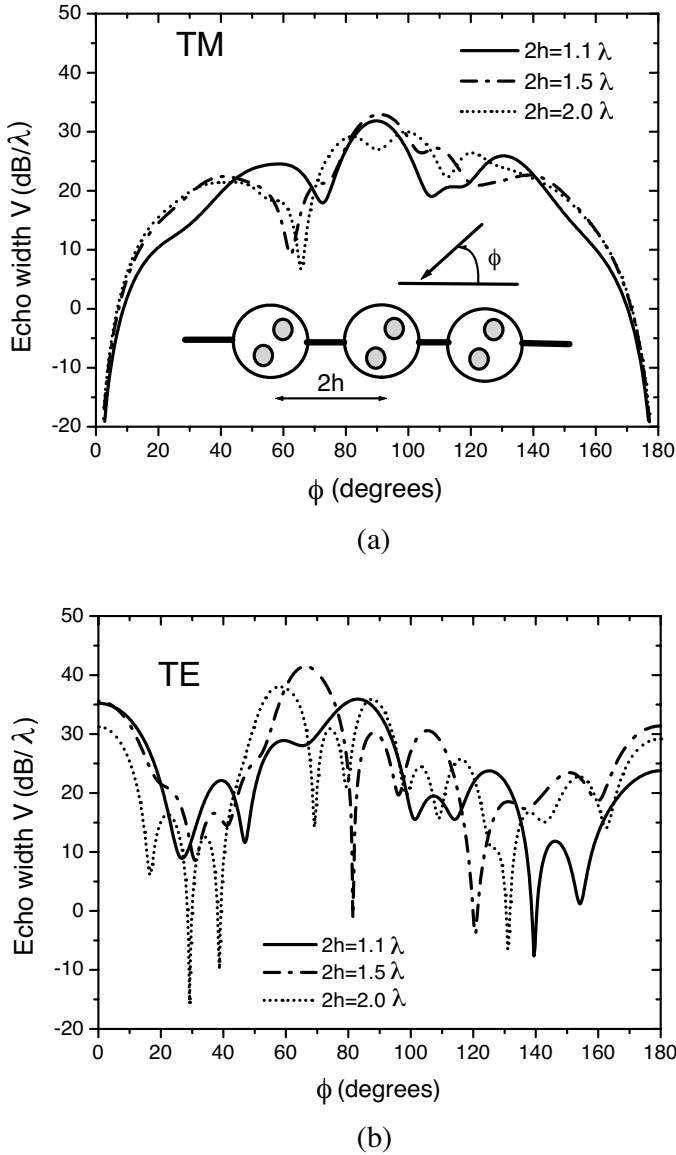


**Figure 9.** Backscattering from three equally spaced, identical parallel channels. The structure of each channel is same to Fig. 8a with  $(\mu_a, \varepsilon_a) = (1.0, 1.0)$ ,  $(\mu_c, \varepsilon_c) = (1.0, 2.0)$ ,  $a = 0.5\lambda$ ,  $d = 0.3\lambda$ ,  $R = 0.1\lambda$ ,  $\alpha = 45^\circ$  (a) TM case (b) TE case.

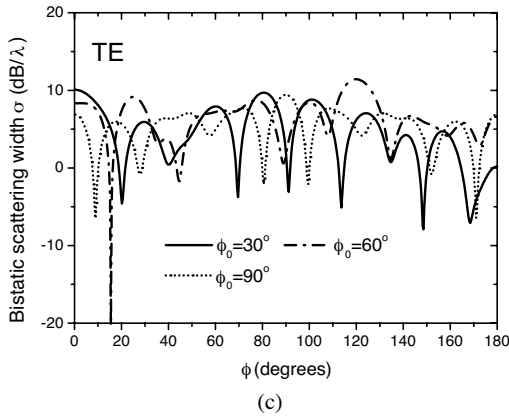
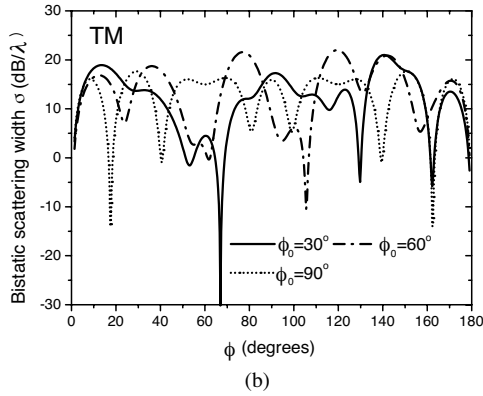
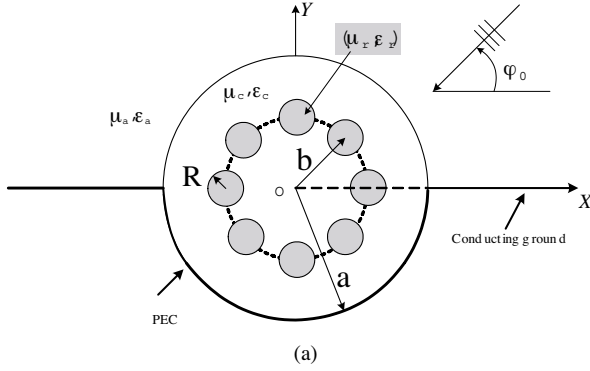


**Figure 10.** The scattering pattern from a semicircular channel with 8 equally spaced circular dielectric cylindrical inclusions.  $(\mu_a, \epsilon_a) = (1.0, 1.0)$ ,  $(\mu_c, \epsilon_c) = (1.0, 2.0)$ ,  $(\mu_r, \epsilon_r) = (1.0, 3.5)$ ,  $a = 2.0\lambda$ ,  $b = 1.0\lambda$ ,  $R = 0.2\lambda$ .

and that of Ref. [5] is, we guess, due to different expansion items or computer precision. We use 21 expansion functions to express the field outside the channel and 41 cylindrical harmonics for the field inside; in addition, double precision is used for all variables and special functions. The aggregated T-matrix method is also validated in Fig. 6 by comparison with iterative solution given in [15] for five conducting cylinders. Moreover, we also simulated scattering from two channels and compared with that published in [8] as shown in Fig. 7. It can be seen that two results agree excellently with each other. These calculations have proved the accuracy of the coupled method proposed in this paper.

Fig. 8(a) gives an illustration of a semicircular channel with two conducting circular cylinders inside. Fig. 8(b) provides the backscattering echo width in vertical direction versus different double-cylinder orientations. It seems that the orientation of inclusive cylinders has greater impact on the echo width of TM wave than that of TE wave. Next example is for backscattering versus incident angle from three identical semicircular channels. The individual channel has the same geometric structure to that shown in Fig. 8(a). The effects of different channel separations on echo width are presented in Fig. 9(a) and (b) for both TM and TE waves. For TM wave incidences in this example, the echo width is not sensitive to the variation of the separation of channels. However, as shown in Fig. 9(b), the various separations of channels result in quite different echo pattern for TE wave case. Fig. 10(a) illustrates the geometry of a semicircular channel with total eight dielectric cylinders inside. It is worth to note that the analysis will become very cumbersome by conventional dual-series eigenfunction solutions. Scattering patterns for different incident angles are provided in Fig. 10(b) and (c) for both TM and TE cases, respectively. The complexity of scattering patterns indicates that there are complicated multiple scattering of EM waves among inclusive cylinders. These numerical examples have shown the advantages of the hybrid method proposed over conventional method in modeling complex semicircular channels.

## 7. CONCLUSIONS

A novel microwave network method is first proposed to derive the T-matrix of a single semicircular channel with several cylindrical inclusions. Then, the addition theorems of cylindrical harmonics in half space are given explicitly and used to take account of multiple scattering effects among parallel channels. This coupled method has greatly simplified the analysis by adopting the divide-and-conquer

strategy and could be implemented step by step. The accuracy of the method is validated by comparing with those results previously published. Much more complex parallel semicircular channels are discussed to show the advantage of this coupled method over the conventional dual-series eigenfunction solutions. Either TM or TE polarization are considered in a similar way. The coupled approach discussed in this paper could easily extend to the analysis of semi-elliptic channels or channels filled with chiral materials.

## REFERENCES

1. Sachdeva, B. K. and R. K. Hurd, "Scattering by a dielectric-loaded trough in a conducting plane," *J. Appl. Phys.*, Vol. 48, No. 4, 1473–1476, 1977.
2. Senior, T. B. A. and J. L. Volakis, "Scattering from gaps and cracks," *IEEE Trans. Antennas Propagate.*, Vol. 37, 744–750, 1989.
3. Hinders, M. K. and A. D. Yaghjian, "Dual-series solution to scattering from a semicircular channel in a ground plane," *IEEE Microwave and Guided Waves Lett.*, Vol. 1, No. 9, 1991.
4. Park, T. J., H. J. Eom, Y. Yamaguchi, W.-M.Boerner, and S. Kozaki, "TE plane wave scattering from a dielectric-loaded semi-circular trough in a conducting plane," *J. Electromagn. Waves Applicat.*, Vol. 7, No. 2, 234–245, 1993.
5. Ragheb, H. A., "Electromagnetic scattering from a coaxial dielectric circular cylinder loading a semicircular gap in a ground plane," *IEEE Trans. Microwave Theory Tech.*, Vol. 43, No. 6, 1303–1309, 1995.
6. Byun, W. J., J. W. Yu, and N. H. Myung, "TM scattering from hollow and dielectric-filled semielliptic channels with arbitrary eccentricity in a perfectly conducting plane," *IEEE Trans. Microwave Theory Tech.*, Vol. 46, No. 9, 1336–1339, 1998.
7. Uslenghi, P. L. E., "Exact penetration, radiation, and scattering for a slotted semielliptical channel filled with isorefractive material," *IEEE Trans. Antennas Propagat.*, Vol. 52, 1473–1480, 2004.
8. Yu, J. W., W. J. Byun, and N. H. Myung, "Multiple scattering from two dielectric-filled semi-circular channels in a conducting plane: TM case," *IEEE Trans. Antennas Propagat.*, Vol. 50, No. 9, 1250–1253, Sep. 2002.
9. Stratigaki, L. G., M. P. Ioannidou, and D. P. Chrissoulidis, "Scattering from a dielectric cylinder with multiple eccentric

- cylindrical dielectric inclusions,” *IEE Proc. Microwave Antenna Propagat.*, Vol. 143, No. 6, 505–511, 1996.
10. Toyama, H., K. Yasumoto, and T. Iwasaki, “Electromagnetic scattering from a dielectric cylinder with multiple eccentric cylindrical inclusions,” *Progress in Electromagnetics Research*, Vol. 40, 113–129, 2003.
  11. Peterson, B., S. Ström, “T-matrix for electromagnetic scattering from an arbitrary number of scatterers and representation of  $E(3)$ ,” *Phys. Rev. D8*, 3661–3678, 1973.
  12. Chew, W. C., Y. M. Wang, and L. Gurel, “Recursive algorithm for wave scattering solutions using windowed addition theorem,” *J. Electromagn. Waves Applicat.*, Vol. 6, No. 11, 1537–1560, 1992.
  13. Chew, W. C., L. Gurel, Y. M. Wang, G. Otto, R. L. Wagner, and Q. H. Liu, “A generalized recursive algorithm for wave-scattering solutions in two dimensions,” *IEEE Trans. Microwave Theory Tech.*, Vol. 40, 716–722, Apr. 1992.
  14. Chew, W. C., *Waves and Fields in Inhomogeneous Media*, Van Nostrand Reinhold, New York, 1990.
  15. Sharkawy, M. A. and A. Z. Elsherbeni, “Electromagnetic scattering from parallel chiral cylinders of circular cross sections using an iterative procedure,” *Progress in Electromagnetics Research*, Vol. 47, 87–110, 2004.
  16. Shen, T., W. Dou, and Z. Sun, “Gaussian beam scattering from a semicircular channel in a conducting plane,” *Progress in Electromagnetics Research*, Vol. 16, 67–85, 1997.

**Yao Jiang Zhang** received B.E. and M.E. degrees in 1991 and 1994 from University of Science & Technology of China, both in Electrical Engineering, Hefei, Anhui, China. In 1999, He received Ph.D. degree in Physical Electronics from Beijing University. From 1999 to 2001, he was with Tsinghua University, Beijing, China, as a Postdoctoral Research Fellow. Since Aug. 2001, he is a senior research engineer in Institute of High Performance Computing (IHPC), Agency for Science, Technology and Research (A\*STAR), Singapore. His current research interests include fast algorithm and parallel computing techniques in computational electromagnetics, numerical simulation of complex electromagnetic materials, photonic crystals and high-speed electronic circuit package.



**Alexander Bauer** born in Karlsruhe, Germany on 26 May 1980. In 2000, he was enrolled, as a Diplom (Master's degree) student, in the Department of Electrical Engineering, University of Karlsruhe, Germany. From June 2004 to November 2004, he was with the Institute of High Performance Computing, Agency for Science, Technology and Research (A\*STAR), as an exchange student under National University of Singapore (NUS). His research interests focus on electromagnetics and wireless communication.

**Er Ping Li** received his MEng from Xi'an Jiaotong University, China and Ph.D. from Sheffield Hallam University, UK both in electrical engineering in 1986 and 1992 respectively. He has been a research fellow and lecturer at Sheffield Hallam University from 1989 to 1992, senior research fellow and project manager in Singapore research institute and private company from 1993 to 1999. In April 2000, he joined Institute of high performance computing at National University of Singapore as a member of technical staff and R&D Manager. Dr. Li is a Senior Member of IEEE and an elected deputy Chairman for IEEE EMC Chapter in Singapore. His research interests include computational electromagnetics, computational nanotechnology, high-speed electronic modeling and EMC/EMI.